5-9-2017

Mapping the Embryological Development of the Temporomandibular Joint with Cone-Beam Computed Tomography

Sonya Kalim
skalim@uchc.edu

Mapping the Embryological Development of the Temporomandibular Joint with Cone-Beam Computed Tomography

Sonya Kalim

B.S., King's College, 2011
D.M.D., Temple University, 2014

A Thesis

Submitted in Partial Fulfillment of the

Requirements for the Degree of

Master of Dental Science

At the

University of Connecticut

2017

APPROVAL PAGE

Masters of Dental Science Thesis

Mapping the Embryological Development of the Temporomandibular Joint with Cone-Beam Computed Tomography

Presented by

Sonya Kalim, B.S., D.M.D.

Major Advisor_____
Alan G. Lurie

Associate Advisor_____
Aditya Tadinada

Associate Advisor_____
Sumit Yadav

University of Connecticut

2017

ACKNOWLEDGEMENTS

This project would not have been feasible without the involvement of several individuals.

Dr. Alan Lurie first approached me about taking on this project and he has been a wonderful advisor, providing me with invaluable guidance and support. This is not only true for this project, but throughout the duration of my residency. Thank you, Dr. Lurie, for always making the time to help me navigate the journey to becoming an OMFR.

This project would not have been possible without the collaboration of Jerry Conlogue and the curators of the specimen collection assessed in this study. Thank you for allowing me to access the specimen collection. Thank you, Jerry, for sharing your passion for this project, contributing all your resources, and making countless trips to UCONN to deliver specimens for imaging and analysis.

I want to thank Dr. Aditya Tadinada for his contributions to this project as well as throughout my residency by being a great source of support and guidance.

I also want to thank Dr. Sumit Yadav for his assistance throughout the duration of this project.

Finally, I'd like to thank my family for their unwavering love and support as I've gone through not only my educational journey, but life in general. They have always been my cheerleaders and I cannot express how grateful I am for them. I love you all!

TABLE OF CONTENTS

ABSTRACT

The duration of time between the 7th and 12th weeks of intrauterine life is the most critical to the development of the temporomandibular joints (TMJs), as the general architecture of the region is established. The formation of the osseous and soft tissue structures are well-documented histologically, but are less so radiographically. This is the first known study to image and analyze the TMJs in fetal specimens of varying weeks of development using cone-beam computed tomography (CBCT). Thirty-one specimens from the Kier/Conlogue Collection at the Cushing Center in the Harvey/Cushing/John Hay Whitney Medical Library at Yale University were evaluated. In this study, we aimed to demarcate the bony components of the TMJs and correlate the amount of ossification in the condylar and temporal components to the week of development using CBCT gray values as a quantitative measure of bone density. The CBCT acquisitions beautifully demonstrated progressive morphologic development of the condylar and temporal components of the TMJ. However, the data analyzed in this study demonstrated that the development of the TMJs varied considerably between specimens and even between TMJs of the same specimen. Thus, gray values did not consistently increase with the week of development as expected and were instead found to be quite variable.

INTRODUCTION

The temporomandibular joints (TMJs) are synovial in nature and are formed by the articulation of the mandible with the cranial base bilaterally[1, 2, 3, 4]. They are unique and distinguishable from other joints of the body in several ways which are related to the morphology of the joint, including function of the joints as a single unit though anatomically separate [3, 4], facilitation of two different types of movements (rotation and translation)[2], and the presence of a thin layer of fibrocartilage along the articular surfaces of the bony components of the joints (rather than hyaline cartilage as in other synovial joints)[1, 4].

More specifically, the TMJs are formed superiorly by the glenoid fossa and articular eminence of the squamous portion of the temporal bone and inferiorly by the condylar process of the mandible on either side[1, 2, 3, 4]. The articular eminence is convex in shape and the glenoid fossa is concave; together they create an "S" shape[4]. The depth of the glenoid fossa varies and the development of the articular eminence is dependent upon normal function of the mandibular condyle[4]. The shape of the mandibular condyle can vary considerably, but in general, it follows an ellipsoid contour[4].

The space between the temporal and condylar components is occupied by the articular disc[1, 2, 3, 4], which is composed of dense, avascular fibrous connective tissue and fibrocartilage[1, 2, 4]. The disc separates this region into superior and inferior cavities[1, 2, 4]. The superior cavity allows for translation (forward gliding), while the inferior cavity allows for rotation[1, 2, 4].

The shape of the disc is "biconcave"[1,4] as it conforms to the structures it lays between. The superior surface of the disc is concave anteriorly, where it sits inferiorly to the articular eminence, and convex posteriorly, where it sits inferiorly to the mandibular fossa[2]. The inferior surface of the disc is concave, as it conforms to the generally ellipsoid shape of the condyle[2].

The disc is thick in its anterior and posterior portions and thin in its central one[1, 4]. The central portion mitigates the articulating actions between the articular eminence and the condyle with movement of the joint[1, 4]. The posterior band attaches to retrodiscal tissues, or the bilaminar zone, which consists of superior and inferior lamellae composed of loose fibrous connective and elastic tissues that enclose an area of vascular tissue[1, 4]. The superior lamella firmly attaches to the posterior surface of the glenoid fossa and the inferior lamella firmly attaches to the posterior surface of the condyle[1, 4]. These tissues are essential for the anterior and posterior movements of the articular disc and condyle upon opening and closing the jaw[4].

The entire joint is encapsulated by connective tissue[1, 3] that aids in stabilization and restriction of movements; this is the articular capsule[2]. It attaches superiorly to the tympanosquamous fissure, the glenoid fossa, and the articular eminence and inferiorly to the neck of the condyle[1, 2, 3]. The anterior band and the medial and lateral boundaries of the articular disc attach to the inner surface of the articular capsule[1, 4]. It is also of note that the inner surface of the articular capsule is lined with a synovial membrane, which secretes synovial fluid to keep the joint lubricated[4].

The lateral ligament reinforces the articular capsule anterolaterally, attaching superiorly to the zygomatic arch and inferiorly to the condylar neck[2, 3]. Other ligaments which aid in stabilization of the joint and restriction of its movements are the sphenomandibular ligament, which extends from the sphenoid spine to the lingula of the mandible and the stylomandibular ligament, which extends from the styloid process to the angle of the mandible[2, 3].

Several muscles work in tandem to guide the movements of the joint in order to maintain the functions of the jaws, such as the major masticatory, suprahyoid, and facial muscles. However, only the major muscles of mastication will be discussed, as these are thought to be

instrumental in guiding the development of the TMJs. The lateral pterygoid muscle has a particularly intimate relationship to the TMJ as it originates from the greater wing of the sphenoid and the lateral surface of the lateral pterygoid plate and inserts directly onto the neck of the condyle, the articular capsule, and in some cases the anterior aspect of the articular disc; it aids in depression, protrusion, and lateral movements of the mandible[2, 3]. The medial pterygoid muscle originates from the medial surface of the lateral pterygoid plate and the tuberosity of the maxilla and inserts onto the medial surfaces of the ramus and angle of the mandible; it aids in elevation, protrusion, and grinding movements of the mandible[2,3]. The temporalis muscle originates from the inferior temporal line and the deep temporal fascia of the temporal fossa and inserts onto the coronoid process and anterior ramus of the mandible; it aids in the elevation and retraction of the mandible as well as maintenance of its rest position[2,3]. Lastly, the masseter muscle originates from the lateral and inferior surfaces of the zygomatic arch and inserts onto the lateral surface of the ramus and angle of the mandible; it aids in the elevation, protrusion, and small grinding movements[2,3].

The embryological development of the TMJs is a complex process, dependent on the normal function and interaction of various embryological tissues. It is very well-defined based on histologic studies, which show that precursor tissues leading to the formation of bone, via intramembranous and endochondral ossification, and cartilage are essential[2,5]. Integral precursor tissues derive from the first pharyngeal arch and include: ectodermal neural crest cells ("ectomesenchyme"), which give rise to the squamous portion of the temporal bone and the mandible, including the condylar and coronoid processes, and mesodermal mesenchyme, which gives rise to the articular disc and the muscles of mastication[2, 5]. As previously mentioned, the development of the masticatory muscles is instrumental, as they are thought to affect the

formation and ossification of the mandibular condyle via tension and constant attachment and reattachment as osseous structures change, with special consideration to the lateral pterygoid muscle[6, 7, 8].

The development of the TMJs begins within the 7th week of intrauterine development and continues on throughout fetal life as well as postnatally into adulthood[7, 9]. However, the period between the 7th and 12th weeks is the most critical to TMJ development[10], as the general architecture of the region is established during this time[11]. At 6 weeks, the development of the mandibular ramus begins with the formation of a bony plate via intramembranous ossification of ectomesenchymal tissue lateral to Meckel's cartilage[7, 8, 12]. It is important to note that Meckel's cartilage is not directly involved with TMJ development; it is suggested that it serves as a scaffold for joint development[9, 12], since it is responsible for the development of the mandibular processes[5]. Development of the temporalis muscle, which eventually attaches to the coronoid process of the mandible within the 7th and 8th weeks, also begins at 6 weeks[13].

At 7 weeks, Meckel's cartilage and the developing ramus are surrounded by ill-defined ectomesenchymal tissue, some of which, within less than a week's time, condenses to form a distinguishable oval-shaped mass that eventually gives rise to the condylar process[9, 13, 14, 15]. Development of the lateral pterygoid muscle also begins at 7 weeks and its attachments to the developing condylar processes and articular disc are evident throughout intrauterine TMJ development[7, 9, 10, 12, 13, 14].

At 8 weeks, the development of the squamous portion of the temporal bone begins as an oval-shaped mass of ectomesenchymal tissue that is located superolaterally to the developing condylar process[10, 11, 14]. Development of the medial pterygoid and masseter muscles also begins at 8 weeks. The medial pterygoid muscle attaches to the inner plate of the angle of the mandible

at 10 weeks and the masseter muscle extends from the developing squamous portion of the temporal bone to the surface of the ramus at 14 weeks[12, 13].

At 9 weeks, the temporal ectomesenchymal tissue elongates to form a "shelf" which will give rise to the zygomatic process and glenoid fossa of the temporal bone via intramembranous bone formation[11, 14]. The temporal component is separated from the condylar process by both a dense band of mesodermal mesenchymal tissue, which eventually gives rise to the articular disc[10], as well as loose mesodermal mesenchymal tissue.[11, 14]. Lastly, the superior aspect of the developing ramus extends into the condylar process[11, 14].

At 10 weeks, secondary cartilage appears within the condylar process, just lateral to the extension of the ramus into the region. Within a week, the secondary cartilage assumes a conical shape, with its apex towards the developing ramus, and the condyle grows via endochondral ossification[6, 7, 10, 11, 12, 14]. As the temporal and condylar components begin to grow towards one another, the dense strip of mesodermal mesenchymal tissue (primitive articular disc) thins and a series of clefts form below it and the condylar head, which eventually coalesce to form the lower joint cavity[7, 12, 13, 14].

At 11 weeks, the lower joint cavity is well-formed, the superior joint cavity is still developing with the formation of several coalescing clefts, and the articular disc is clearly distinguished[10, 11, 12, 14, 15]. Ectomesenchymal tissue within the temporal component extends to the lateral aspects of the condylar process and the articular disc, the first indication of a joint capsule[7, 14].

At 12 weeks, there is a tremendous increase in size of all structures: there is increased bone growth within the both temporal and condylar components and the joint cavities are fully formed[11,14]. At this stage, the glenoid fossa of the temporal bone has acquired a slightly concave

shape and is larger than the articular surface of the condyle[11,14]. In addition, vascular mesenchyme appears within the condylar cartilage[14].

In the following weeks of fetal development, there is an increase in overall size of the various TMJ components, further development of vessels and nerves, formation of bone trabecula, marrow spaces, and hematopoietic cells, maturation of the fibers of the masticatory muscles, and development of synovial tissues[6-15]. There is a reduction of Meckel's cartilage until it eventually disappears[9, 11]. The only remnant of Meckel's cartilage is the sphenomandibular ligament[5]. The secondary cartilage within the condylar process diminishes until a thin layer remains on the articular surface of the condyle[7]. The tissue within this layer as well as in the articular disc develops a fibrous character, with high collagen I and II content[7]. It is also of note that the articular eminence does not form prenatally, but rather postnatally by 6 years, at which time the articular disc shape adjusts to the change in morphology[7].

As previously mentioned, most studies that have previously been done regarding the development of the TMJs are based on histological sections of human fetuses of varying weeks. However, Sato et al.[6] and Morimoto et al.[9] imaged their fetal specimens (ranging from 12 weeks to term) with low voltage plain radiographs to evaluate which structures could be visualized. Both studies found that the osseous components of the TMJ could be described from 16 weeks and on, though Sato et al.[6] found the zygomatic arch and the glenoid fossa of the temporal bone, the condylar process, and the coronoid process were distinguishable at 12 weeks.

Although previous studies have used histological sections to create 3-dimensional computer reconstructions as an aid for the visualization of prenatal TMJ development[10, 13], currently, no fetal specimens have been imaged by a 3-dimensional imaging modality, such as multi-detector computed tomography (MDCT) or cone-beam computed tomography (CBCT) for

this purpose. Both types of CT offer high-resolution, multi-planar imaging and provide flexibility in the use of acquisition parameters, as operators may adjust the field-of-view (FOV), tube voltage (kV), and tube current (mA), which together influence the quality and contrast of the images acquired[16]. The ability to change acquisition parameters readily is an advantage, as imaging of each individual fetal specimen can be optimized. However, CBCT allows for the use of smaller voxel sizes during scan acquisition in comparison to MDCT[4, 16]. Voxel sizes of 240 microns can be achieved with MDCT, whereas voxel sizes as low as 80 microns can be achieved with some CBCT machines[4, 16]. Essentially, CBCT scans offer superior spatial resolution, which is an advantage for imaging small, mineralized anatomical structures. This suggests that CBCT has superior capability than MDCT to effectively demarcate the osseous components of the developing TMJ in fetal specimens, which vary widely in size and degree of mineralization, depending on the stage of development.

However, it has been suggested that CBCT does not offer a reliable method to assess tissue densities quantitatively. The ability of a CBCT unit to display differences in attenuation of the x-ray beam is directly linked the bit depth of the detector, which determines the number of shades of gray available to display contrast differences due to attenuation[4]. Currently, all detectors utilized in CBCT units are capable of 12 bits or more[4]. This means that the gray scale is determined by the manufacturer and is not calibrated using a reference scale with pre-determined qualitative values for different tissues or compounds, such as water[17, 18].

In contrast, such a reference scale is used for the MDCT modality, where the linear attenuation coefficient values (fraction of attenuated photons per unit thickness of a material) of each tissue, water, and air is taken into account[18, 19] to create a quantitative unit that represents the tissue density that is proportional to the degree to which the material within the voxel

attenuates the x-ray beam; this is known as the Hounsfield unit (HU)[4, 18, 20]. This means that HUs demonstrated by MDCT viewing software correspond with gray values viewed on the computer display after image reconstruction[18, 19] and provide accurate quantitative assessments of different tissue densities[21, 22]. This may not be true in regards to gray value measurements demonstrated by CBCT viewing software[20, 22].

There are considerable differences in the various types of CBCT units, including exposure parameters, FOV capabilities, hardware components, reconstruction algorithms, etc.[18] which make it extremely difficult to standardize a method to scale gray values during the reconstruction process[22]. Additionally, CBCT systems are subject to inherent artifacts which can affect the consistency of gray values demonstrated on a computer display by degradation of the images produced[4, 18, 19], which namely includes image noise that may be caused by scatter radiation, divergence of the x-ray beam, defective detector pixels, and non-uniformity of the x-ray beam (Heel effect) as well as partial volume averaging, which designates an average gray value of different densities captured by the detector pixel to the reconstructed voxel because the structures imaged were smaller than the voxel size[4, 18]. Partial volume averaging is evident in MDCT as well[4].

Despite these obstacles, several studies have shown that although gray value measurements recorded from CBCT scans were consistently higher than the HU measurements recorded from MDCT scans in regards to bone density, the values were similar and that there was a linear correlation between gray values demonstrated by CBCT and HU values demonstrated by MDCT[17, 19-27]. This suggests that CBCT has the potential to accurately assess bone density. Taking into consideration that CBCT is an effective modality in assessing bony contours and can provide a quantitative assessment of bone density, it is possible to not only

distinguish the bony components of the TMJs, but also to correlate the amount of ossification within them to the week of fetal development using CBCT gray values.

OBJECTIVES

The objective of this study was to demarcate the bony components of the TMJs in fetal specimens of varying weeks of development and quantify amount of ossification in the condylar and temporal components with regard to age using the CBCT modality.

SPECIFIC AIMS

1. Determine diagnostic acquisition parameters for the CBCT imaging of each specimen,
2. Demarcate the bony components of the TMJs,
3. Record gray value measurements at standardized points within the temporal and condylar bony components and correlate these values to the week of development,
4. Provide data about TMJ embryology and development in the human fetus.

HYPOTHESES

1. Each specimen would have a different optimal set of acquisition parameters based on the degree of mineralization indicated by the week of development.
2. Bony components of the TMJs would be well-distinguished on CBCT images.
3. Gray value measurements of the bony components of the TMJs would increase with the week of development, indicating an increased amount of ossification, consistent with the normal development of the TMJs.

MATERIALS AND METHODS

Due to the anonymity of the specimens in the collection examined in this study, approval from the Institutional Review Board was waived. In this descriptive study, 31 dry fetal skulls varying from 11 to 38 weeks of development from the Kier/Conlogue Collection at the Cushing Center in the Harvey/Cushing/John Hay Whitney Medical Library at Yale University were imaged with the J. Morita 3D Accuitomo 170 CBCT unit (J. Morita USA, Irvine, CA). Scout images of each skull were taken with 80 kV and 2 mA and were positioned using the midline, mandibular condyle, and the supraorbital ridge as anatomical landmarks. Each skull was then imaged with identical acquisition parameters with the exception of the field-of-view (FOV). Smaller skulls were imaged with a 40x40mm FOV (80 micron voxels) and larger skulls were imaged with a 60x60mm FOV (125 micron voxels). The FOV was centered on the region of the TMJ in each scan. Each skull was imaged using 9 parameter settings in high resolution mode with a 360^{o} trajectory arc. Parameter settings included: 60 kV and 1 mA, 60 kV and 4.5 mA, 60 kV and 8 mA, 75 kV and 1 mA, 75 kV and 4.5 mA, 75 kV and 8 mA, 90 kV and 1 mA, 90 kV and 4.5 mA, and 90 kV and 8 mA.

Once acquired, the scans were viewed using Anatomage InVivo5 dental software and evaluated for diagnostic value. The most diagnostic scan was chosen based on the least amount of noise ("graininess") captured within the scan. If two scans were similar in quality, the one acquired with a higher kV was chosen, as lower contrast is demonstrated and slight differences in density could be more readily detected. One acquisition parameter was chosen for all of the skulls (90 kV and 4.5 mA).

A total of 57 TMJs were analyzed, as 5 skulls were missing a condylar process on one side. Gray values were taken at the center and superior, medial, and lateral poles of the

mandibular condyle and the center of the glenoid fossa directly above the center of the condyle (Figure 1). They were taken using the pinpoint feature, which indicates the same location precisely on all multiplanar views (Figure 2). The gray values of the pinpoints on each of the axial, sagittal, and coronal sections were recorded and averaged. All measurements were taken on the same laptop computer to ensure standardization of the gray scale.

Figure 1. Points at which gray values were recorded as depicted on a coronal section.

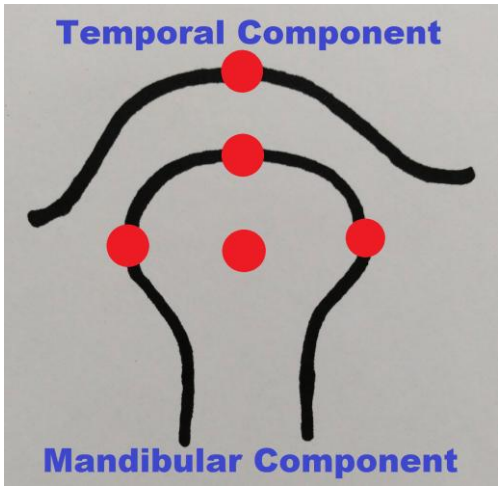

Figure 2. Pinpoint feature used to record gray values.

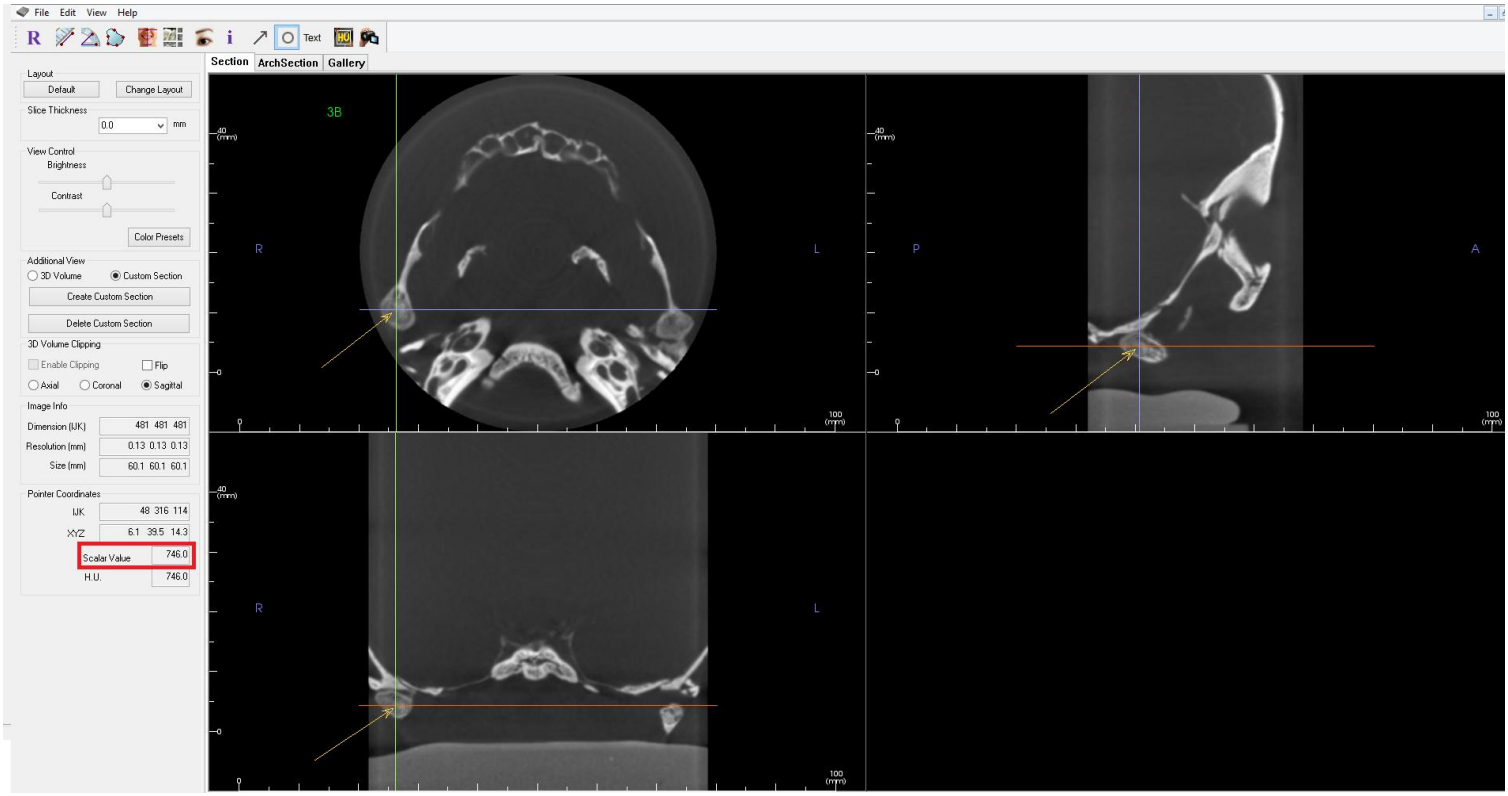

RESULTS

It was found that all mineralized components of the specimens were well-demarcated on CBCT images as expected, including the TMJs. The week or range of weeks of development was/were known prior to data analysis. Upon analysis of the TMJs, it was found that there was great variability between the condylar components of the TMJs independent of week of development. In some specimens, there were differences in morphology between the right and left sides. The specimens varied most notably in regards to size, cortical boundaries, and degree of trabecular bone fill. In general, the condylar component increased in size with an increase in week of development. Please refer to Table 1 for specific data about each specimen. However, it is of note that the appearances of the temporal components of the TMJs remained consistent on imaging. In all specimens, the glenoid fossae appeared flat and smooth without any or with a slight concavity and the articular eminence was not present. This radiographic appearance is in accordance with the histologic development previously discussed.

Table 1. Descriptions of the condylar components of the TMJs associated with each specimen in order of week of development.

Skull	Age	Description
#4247	11 weeks	R condyle: extremely small with very little bone fill and sparsely thin cortices L condyle: not measureable as only fragments are present
#X165	12 weeks	R & L condyles: small with robust bone fill and distinguishable uniform cortices, with more robust medial and lateral cortices that are more robust on the R side
#50	12 weeks	R & L condyles: very small, thin, dense, and indistinguishable cortices
#14	12 weeks	R condyle: small with very little bone fill and well-defined, dense, irregular cortices L condyle: not measureable as only fragments are present
#16R	13 weeks	R & L condyles: small, thin, and dense with irregular, non-uniform cortices that are more robust on the medial poles

#26	13 weeks	R & L condyles: very small, thin, dense with indistinguishable cortices
#3A	14 weeks	L condyle: small, with very little bone fill with well-defined, dense cortices R condyle: not measureable as only fragments are present
#1A	14 weeks	R & L condyles: small, thin, dense with indistinguishable cortices
#43	14 weeks	R & L condyles: small with moderate bone fill and distinguishable, thin, uniform cortices
#158996	14 weeks	R & L condyles: very small, thin, dense with indistinguishable cortices
#10	15 weeks	R & L condyles: very small, thin, dense with indistinguishable cortices
#13	15 weeks	R condyle: large with porous bone fill and irregular cortices of varying thicknesses L condyle: very small, thin with dense bone fill and indistinguishable cortices
#21567	16 weeks	R & L condyles: small with dense bone fill and indistinguishable cortices
#42467	16 weeks	R & L condyles: very small, thin, and dense with indistinguishable cortices
A	16 weeks	R condyle: small with robust bone fill and distinguishable cortices of varying thicknesses (with the medial pole being more robust than the lateral pole) L condyle: small with dense bone fill and indistinguishable cortices
#12	16 weeks	R condyle: small with robust bone fill and distinguishable, uniform cortices L condyle: small with dense bone fill and indistinguishable cortices
CS-1	16 weeks	R & L condyles: small, thin, and dense with indistinguishable cortices
#3842B	16-18 weeks	R & L condyles: small with porous bone fill and irregular, non-uniform cortices with varying thicknesses
#127992	16-18 weeks	R & L condyles: small with very little bone fill and distinguishable, uniform cortices
#9519	16-18 weeks	R & L condyles: moderate with minimal bone fill and distinguishable, thin, uniform cortices
#16WRS/2.2	18 weeks	R & L condyles: small with robust bone fill and uniform thin cortices

#74	18 weeks	R & L condyles: very small, thin, and dense with indistinguishable cortices
#42767	18 weeks	R & L condyles: very small, thin, and dense with indistinguishable cortices
#18	20-22 weeks	L condyle: moderate with moderate bone fill and distinguishable, uniform cortex on the medial pole and missing cortex on the lateral pole R condyle: not measureable as only fragments are present
#7/4148	20-22 weeks	R & L condyles: small, with little bone fill and thin uniform cortices with more robust cortices on the R side
#5	20 - 28 weeks	R condyle: moderate with porous bone fill and thin uniform cortices L condyle: not measureable as only fragments are present
#6	26-30 weeks	R & L condyles: moderate with porous bone fill and irregular, non-uniform cortices with varying thicknesses (medial pole cortex thinner than the lateral pole; R side more robust than L)
#4	26 weeks	R & L condyles: large with robust bone fill and irregular, non-uniform cortices with varying thicknesses
#3	32-36 weeks	R & L condyles: large with porous bone fill and distinguishable non-uniform cortices with varying thicknesses
#2	32-38 weeks	R & L condyles: large with porous bone fill and irregular, non-uniform cortices with varying thicknesses
#3B	32-38 weeks	R & L condyles: large with porous bone fill and thin uniform cortices

As a result of the variability amongst specimens, gray value measurements taken at the designated points on the temporal and mandibular components were not consistently greater with estimated week of development as hypothesized. Additionally, gray values at certain designated points could not be recorded in many specimens due to TMJ morphology. In 20 of the specimens, measurements at the superior aspect of the mandibular condyle were excluded, as a distinction between the temporal component and the condylar component could not be made. In 10 of the specimens, measurements at the medial and lateral poles of the mandibular condyle were excluded, as a distinction between a cortical boundary and trabecular bone could not be

made. It is of note that the gray values recorded at each point were consistent with bone density as was expected, in that higher gray values were recorded for bone appearing more dense, such as at condylar cortical boundaries and the glenoid fossae, and lower values were recorded for bone appearing less dense, such as where trabecular bone was found. Please see Table 2 for gray value measurements taken for each specimen.

Table 2. Recorded average gray values for each specimen in order of week of development.

[1]AGV = average gray value; [2]CMC = center of the mandibular condyle; [3]SMC = superior pole of the mandibular condyle; [4]CGF = center of the glenoid fossa; [5]LMC = lateral pole of the mandibular condyle; [6]MMC = medial pole of the mandibular condyle

Skull	Age	AGV[1] at CMC[2]	AGV[1] at SMC[3]	AGV[1] at CGF[4]	AGV[1] at LMC[5]	AGV[1] at MMC[6]
#4247 R TMJ	11 weeks	223	none	547	none	none
#X165 R TMJ	12 weeks	971	none	1052	958	928
L TMJ		967	none	1053	852	730
#50 R TMJ	12 weeks	1223	none	1098	none	none
L TMJ		1011	none	1155	none	none
#14 R TMJ	12 weeks	263	none	1170	575	767
#16R R TMJ	13 weeks	509	none	960	844	966
L TMJ		574	none	1045	536	777
#26 R TMJ	13 weeks	1251	none	1260	none	none
L TMJ		1257	none	1210	none	none
#3A L TMJ	14 weeks	535	none	1174	1098	937

#1A R TMJ	14 weeks	931	none	932	731	829
L TMJ		975	none	988	886	854
#43 R TMJ	14 weeks	356	none	879	507	949
L TMJ		421	none	1045	621	629
#158996 R TMJ	14 weeks	985	none	1005	none	none
L TMJ		949	none	1006	none	none
#10 R TMJ	15 weeks	574	none	906	none	none
L TMJ		850	none	861	none	none
#13 R TMJ	15 weeks	664	none	893	777	1260
L TMJ		1140	none	1311	none	none
#21567 R TMJ	16 weeks	813	579	831	519	660
L TMJ		749	781	782	642	722
#42467 R TMJ	16 weeks	831	none	991	none	none
L TMJ		832	none	933	none	none
A R TMJ	16 weeks	807	none	1062	663	1026
L TMJ		962	none	961	944	921
#12 R TMJ	16 weeks	763	none	949	778	782
L TMJ		890	none	969	760	733
CS-1 R TMJ	16 weeks	760	none	827	none	none
L TMJ		830	none	822	none	none

#3842B R TMJ	16-18 weeks	105	none	966	388	587
L TMJ		127	none	1039	643	515
#127992 R TMJ	16-18 weeks	30	527	837	374	759
L TMJ		30	473	698	453	895
#9519 R TMJ	16-18 weeks	480	612	1041	752	471
L TMJ		359	949	1568	593	1058
#16WRS/2.2 R TMJ	18 weeks	554	820	1538	633	849
L TMJ		613	1006	1532	634	894
#74 R TMJ	18 weeks	623	none	1173	none	none
L TMJ		952	none	1050	none	none
#42767 R TMJ	18 weeks	848	none	829	none	none
L TMJ		985	none	1028	none	none
#18 L TMJ	20-22 weeks	399	872	1348	413	730
#7/4148 R TMJ	20-22 weeks	312	none	845	830	781
L TMJ		217	none	877	562	595
#5 R TMJ	20 - 28 weeks	270	733	927	714	645
#6 R TMJ	26-30 weeks	395	882	1642	1021	654
L TMJ		874	871	1457	911	655
#4 R TMJ	26 weeks	634	524	781	1092	1085
L TMJ		424	791	1030	1082	1034

#3 R TMJ	32-36 weeks	702	720	1307	530	884
L TMJ		709	690	1429	638	1240
#2 R TMJ	32-38 weeks	257	563	978	796	723
L TMJ		157	1043	897	1020	612
#3B R TMJ	32-38 weeks	750	633	1327	633	871
L TMJ		757	697	1465	545	756

Due to the small sample size, the variable nature of the specimens, and the inability to compare images and measurements taken in the present study with another study, we thought a descriptive analysis would be more appropriate than parametric statistical testing. Please refer to Table 2 for abbreviations.

One specimen was aged at 11 weeks with an AGV at the CMC of 223 and an AVG at the CGF of 547. There is no range of AGVs as only the right TMJ was analyzed. No other measurements were taken for this specimen. Three specimens were aged at 12 weeks with AGVs of 263-1223 at the CMC, 1052-1170 at the CGF, 575-958 at the LMC, and 730-928 at the MMC. AGVs for the SMC were not recorded in any of these specimens. Two specimens were aged at 13 weeks with AGVs of 509-1257 at the CMC, 960-1260 at the CGF, 536-844 at the LMC, and 777-966 at the MMC. AGVs for the SMC were not recorded in any of these specimens. Four specimens were aged at 14 weeks with AGVs of 421-985 at the CMC, 879-1174 at the CGF, 507-1098 at the LMC, and 629-949 at the MMC. AGVs for the SMC were not recorded in any of these specimens. Two specimens were aged at 15 weeks with AGVs of 574-1140 at the CMC, 861-1311 at the CGF, 777 at the LMC, and 1260 at the MMC. There is no range of AGVs for the LMC and MMC because these points could only be measured for 1 of the 4 TMJs analyzed in

this age cohort. AGVs for the SMC were not recorded in any of these specimens. Five specimens were aged at 16 weeks with AGVs of 749-962 at the CMC, 579-781 at the SMC, 782-1062 at the CGF, 519-944 at the LMC, and 660-1026 at the MMC. Three specimens were aged from 16 to 18 weeks with AGVs of 30-480 at the CMC, 473-949 at the SMC, 698-1568 at the CGF, 374-752 at the LMC, and 471-1058 at the MMC. Three specimens were aged from 18 weeks with AGVs of 554-985 at the CMC, 820-1006 at the SMC, 892-1538 at the CGF, 633-634 at the LMC, and 849-894 at the MMC. Five specimens were aged from 20 to 30 weeks with AGVs of 270-874 at the CMC, 524-882 at the SMC, 781-1642 at the CGF, 413-1092 at the LMC, and 595-1085 at the MMC. Three specimens were aged from 32 to 38 weeks with AGVs of 157-757 at the CMC, 563-1043 at the SMC, 897-1465 at the CGF, 530-1020 at the LMC, and 612-1240 at the MMC. Irrespective of age, the AGVs varied from 30-1257 at the CMC, 473-1043 at the SMC, 822-1538 at the CGF, 374-1098 at the LMC, and 471-1260 at the MMC.

Table 3. Summary of ranges of AGVs for each designated data point with regard to age group.

Age Group	Number of Specimens	AGV Range at CMC	AGV Range at SMC	AGV Range at CGF	AGV Range at LMC	AGV Range at MMC
11 weeks	1	223	N/A	547	N/A	N/A
12 weeks	3	263-1223	N/A	1052-1170	575-958	730-928
13 weeks	2	509-1257	N/A	960-1260	536-844	777-966
14 weeks	4	421-985	N/A	879-1174	507-1098	629-949
15 weeks	2	574-1140	N/A	861-1311	777	1260
16 weeks	5	749-962	579-781	782-1062	519-944	660-1026
16-18 weeks	3	30-480	473-949	698-1568	374-752	471-1058
18 weeks	3	554-985	820-1006	892-1538	633-634	849-894
20-30 weeks	5	270-874	524-882	781-1642	413-1092	595-1085
32-38 weeks	3	157-757	563-1043	897-1465	530-1020	612-1240
11-38 weeks	**31**	**30-1257**	**473-1043**	**822-1538**	**374-1098**	**471-1260**

These gray values suggest that there is great variation in the degree of ossification within the TMJs in this particular specimen collection. There were prominent differences between the

condylar morphologies of the TMJs of each specimen that affected the gray values recorded; this concept applies even to specimens estimated to be the same age (please see Table 1 for reference). Gray values changed dramatically based on the thickness of cortices and type of bone fill (i.e. robust vs. porous); this would suggest that measurement of different standardized points than those indicated in this study, perhaps even a millimeter apart, may have yielded different gray values. It is also worth noting that although there was variation in the gray values recorded with regard to the temporal components (CGF), the gray values were consistently similar or greater in comparison to the measurements taken at other points (CMC, SMC, LMC, and MMC) within each specimen.

DISCUSSION

The primary objectives of this study were to provide data about TMJ embryology radiographically using the CBCT modality and to quantitatively assess the amount of ossification of the bony components of the TMJs in relation to week of development. The motivation for conducting this study incorporates the desire to provide more information about TMJ development radiographically, as most studies previously conducted are histologic in nature. Additionally, in-utero fetuses are not imaged in clinical practice, and thus, the dry skull specimens imaged in this study have the potential to provide insight into TMJ development in-utero.

Firstly, we hypothesized that each specimen would have a different optimal set of acquisition parameters based on the degree of mineralization indicated by the week of development. In this study, this was not the case. All specimens were imaged using standardized parameters, with the only differences being in FOV, which was chosen based on the size of the specimen at the time of imaging. Only the images of a single parameter did not provide any diagnostic information in regards to all specimens (90 kV with 8 mA); otherwise, the TMJs were clearly visualized on the images from all other parameters. This is likely because the removal of soft tissues and preservation of only bony structures eliminates the need to have a longer gray scale in order to differentiate between soft tissues, although a longer gray scale would allow subtle differentiation between mineralized structures as well. Thus, the scan with the least amount of noise (and the longest gray scale) was chosen, which remained consistent throughout data analysis (90 kV with 4.5 mA).

Secondly, we hypothesized that the bony components of the TMJs could be well-distinguished on CBCT images. In this study, this was indeed true; in fact, all of the mineralized

anatomical structures present in each specimen were well-demarcated. The smallest FOV that was capable of imaging the TMJs in full was used, which indicates that the smallest voxel size possible was utilized and that the images were of high resolution. Additionally, the scans were taken in high resolution ("hi-res") mode with a 360^{o} trajectory arc, both of which indicate that a higher amount of base images were taken before reconstruction of the volumetric data. This also improves the spatial resolution. It should be noted, however, that in some specimens, a distinction could not be made between the articulating surface of the glenoid fossa of the temporal bone and the superior pole of the mandibular condyle. We do not attribute this to limitations of the CBCT modality, but rather to the morphology of individual TMJs and/or the method of preservation of the specimens.

Thirdly, we hypothesized that gray value measurements of the bony components of the TMJs would increase with the week of development, indicating an increased amount of ossification, consistent with the normal development of the TMJs. In this study, this was not the case. This may be due to a multitude of reasons pertaining to the specimens as well as the imaging modality utilized. Most importantly, there is very little documented data provided about the previous history of the specimens and how they came to be in their current conditions. The preservation methods utilized are unclear at best, though according to notes recovered from the original researchers of the collection, it is known that they were initially immersed in water for a period between three to five weeks, after which the soft tissues were removed with forceps and scissors. After soft tissue removal, the specimens were immersed in 3% hydrogen peroxide for one to three days depending on the age of the fetus and then rinsed under tap water and dried.

Data about the handling of the specimens after this process is unknown. Many of the specimens had evidence of adhesive materials, such as an unspecified/unknown type of glue,

presumably to adhere the bony components so as to keep the specimens intact. This adhesive material appeared to be present in many specimens specifically adhering the mandibular condyles to the glenoid fossae. It is possible that the adhesive materials used would distort the images rendered by the CBCT machine if determined radiopaque on imaging. This could explain the reason for which the temporal and condylar components could not be distinguished at their articulation in some specimens as previously mentioned. Additionally, it is not known how much, if any, data was lost in the process of preservation. It is suggested that dried fetal specimens shrink and distort as a result of the drying process. It is also possible that data was lost as a result to damage incurred after the drying process, such as chips and fractures.

The week of development for each of the smaller specimens was determined using different source materials and may be inaccurate. Many of the ages of the smaller specimens were determined by the notes recovered by the original researchers of the collection. How ages were determined is unclear. There is some indication that the specimens were aged based on information given by the mother rather than a quantitative assessment, such as crown-rump measurements. Additionally, it does not appear from the records provided that the manner in which the specimens were identified was systematic. This is evident in discrepancies found between the coding written on the containers housing the specimens and coding found on the list of specimens provided. Some of the specimens imaged were not found on the list of specimens at all, but these had ages written on their housing containers. It is unknown if these ages were also obtained by information given by the mother. On the contrary, the age ranges of the larger specimens in the collection were determined by anthropologist Dr. Jaime Ullinger and a student of hers, Michael Strazik, at Quinnipiac University, by analysis of measurements taken between

several different anatomic landmarks. The smaller specimens of the collection were not aged as conventional calipers are not appropriate to measure such small structures.

Even though this collection was initially presented as “normal development”, there were several skulls that had overt, pronounced abnormalities. Some of the specimens showed craniosynostoses, or premature fusion of the cranial sutures, which can sometimes be incompatible with life, depending on the type and severity. It is unknown whether or not a craniosynostosis would affect the development of the TMJ, but this may explain differences in morphology that are not attributable simply to individual differences (i.e. development may have halted earlier than the estimated age). Other specimens had marked hypoplastic or aplastic development of gnathic bones and teeth. Finally, another factor that was not addressed in this study was the assumed gender of the fetus. It would be interesting to see if there were specific differences in morphology in accordance with gender.

Although the use of CBCT and dental software to measure bone density is controversial, in this study, the unpredictability of the gray values is likely more attributable to the differences in TMJ morphology and the preparation and preservation of each specimen rather than the measurements themselves. This is especially indicated by the consistency in the dense structures having higher AGVs and less dense structures having lower AGVs. However, it would be interesting to image these specimens with MDCT and measure HUs at the designated points in order to compare values so as to measure the efficacy of CBCT in measuring bone density.

In conclusion, CBCT clearly images mineralized structures in very early-development human fetuses. There were limitations regarding the collection of specimens that were utilized for this study that could not be avoided. Furthermore, it is likely that fetal specimens from other collections would have the same types of limitations. However, we were able to demonstrate

CBCT as an effective method of imaging fetal specimens and to provide information of clinical significance regarding development of the TMJs. We found that in correlation with histologic development 1) the size of the condylar and temporal components and the amount of trabecular bone within the condylar component increases with further development and increased age, 2) the temporal component remains generally flat throughout intra-uterine life, and 3) the articular eminence remains absent throughout intra-uterine life. We also found that similar to clinical situations, TMJ morphology varies greatly in radiographic appearance, especially in regards to the mandibular condyle.

CONCLUSIONS

This study was the first of its kind in that fetal specimens have not been imaged previously using CBCT. Although our findings on bone density were not statistically significant, we were able to provide radiographic information about fetal specimens, and more specifically, the TMJs, that may provide insight into clinical practice, which is that although the histologic development may be consistent, based on the information provided by this particular collection of specimens, the radiographic appearances of TMJ development vary between individuals and cannot be predicted exactly. In addition, this study demonstrated that genetic abnormalities affecting the development of the craniofacial skeleton have an unknown effect on the development of the TMJ.

FUTURE DIRECTIONS

This collection has provided an extraordinary and unique opportunity to study human fetal skeletal development. CBCT appears to be a powerful method to examine such small mineralized structures. Future studies could well utilize the superb spatial resolution of CBCT to study the morphologic development, and possibly progressive mineralization, of various cranial structures, especially those in the temporal and sphenoid bones of the cranial base and their contents.

Additionally, this particular study is part of a larger ongoing study in which the specimens are imaged using several different modalities. As previously mentioned, some of these specimens have been aged anthropologically, however, another set of structures that can be used for this very purpose is the dentition. It would be interesting to create a study that compares the estimated anthropological age with the age estimated by the development of teeth in order to see if they are in accordance.

As previously mentioned, some other studies that can be done using the data collected in this study would be to compare TMJ morphology differences between males and females and to compare the CBCT gray values collected to MDCT HU values collected from the same designated points in order to gauge the accuracy of using CBCT to measure bone density.

REFERENCES

1. Som, P. M. And Curtin, H. D. Head and neck imaging, volume 1. 5th Edition. St. Louis, Missouri: Elsevier Mosby, 2011.
2. Bogart, B. I. and Ort, V. H. Elsevier's Integrated Anatomy and Embryology. Philadelphia, PA: Mosby Elsevier, 2007.
3. Gilroy, A. M., MacPherson, B. R., Ross, Lawrence, M. R., et al. Atlas of anatomy. 2nd Edition. New York, NY: Thieme Medical Publishers, 2012.
4. White, S. C. and Pharoah, M. J. W. Oral radiology: principles and interpretation. 7th Edition. St. Louis, MO: Elsevier Mosby, 2014.
5. Sadler, T. W. Langman's Medical Embrology. 13th Edition. Philadelphia, PA: Wolters Kluwer, 2015.
6. Sato, I., Ishikawa, H., Shimada, K., et al. Morphology and analysis of the development of the human temporomandibular joint and masticatory muscle. Acta Anatomica, 49: 55-62, 1994.
7. Keith, D. A. Development of the human temporomandibular joint. British Journal of Oral Surgery, 20: 217-224, 1982.
8. Alves, N. Study about the development of the temporomandibular joint in the human fetuses. International Journal of Morphology, 26(2): 309-312, 2008.
9. Morimoto, K., Hashimoto, N., and Suetsugu, T. Prenatal developmental process of human temporomandibular joint. Journal of Prosthetic Dentistry, 57(6): 723-730, 1987.
10. Radlanski, R. J., Lieck, S., and Bontschev, N.E. Development of the human temporomandibular joint. Computer-aided 3D-reconstructions. European Journal of Oral Science, 107: 25-34, 1999.

11. Merida-Velasco, J.R., Rodriguez-Vasquez, J.F., Merida-Velasco, J.A., et al. Development of the human temporomandibular joint. The Anatomical Record, 255: 20-33, 1999.

12. Furstman, L. The early development of the human temporomandibular joint. American Journal of Orthodontics and Dentofacial Orthopedics, 49(9): 672-682, 1963.

13. Ogutcen-Toller, M. and Keskin, M. Computerized 3-dimensional study of the embryologic development of the human masticatory muscles and temporomandibular joint. Journal of Oral and Maxillofacial Surgery, 58: 1381-1386, 2000.

14. Symons, N. B. B. The development of the human mandibular joint. Journal of Anatomy, 86(3): 326-332, 1952.

15. Ogutcen-Toller, M. and Juniper, R. The embryologic development of the human lateral pterygoid muscle and its relationships with the temporomandibular joint disc and meckel's cartilage. Journal of Oral and Maxillofacial Surgery, 51: 772-778, 1993.

16. Spin-Neto, R., Gotfredsen, E., and Wenzel, A. Impact of voxel size variation on CBCT-based diagnostic outcome in dentistry: a systematic review. Journal of Digital Imaging, 26: 813-820, 2012.

17. Cassetta, M., Stefanelli, L. V., Pacifici, A., et al. How accurate is CBCT in measuring bone density? A comparative CBCT-CT in vitro study. Clinical Implant Dentistry and Related Research, 16: 471-478, 2014.

18. Pauwels, R., Jacobs, R., Singer, S. R., et al. CBCT-based bone quality assessment: are hounsfield units applicable? Dentomaxillofacial Radiology, 44: 1-16, 2015.

19. Molteni, R. Prospects and challenges of rendering tissue density in hounsfield units for cone beam computed tomography. Oral Surgery Oral Medicine Oral Pathology Oral Radiology, 116: 105-119, 2013.

20. Razi, T., Niknami, M., and Ghazani, F. A. Relationship between hounsfield unit in CT scan and gray scale in CBCT. Journal of Dental Research, Dental Clinics, Dental Prospects, 8: 107-110, 2014.

21. Kim, D. Can dental cone beam computed tomography assess bone mineral density? Journal of Bone Metabolism, 21: 117-126, 2014.

22. Mah, P., Reeves, T. E., and McDavid, W. D. Deriving hounsfield units using grey levels in cone beam computed tomography. Dentomaxillofacial Radiology, 39: 323-335, 2010.

23. Aranyarachkul, P., Caruso, J., Gantes, B, et. al. Bone density assessments of dental implant sites: 2. Quantitative cone-beam compterized tomography. International Journal of Oral and Maxillofacial Implants, 20: 416-424, 2005.

24. Naitoh, M., Hirukawa, A., Katsumata, A., et al. Evaluation of voxel values in mandibular cancellous bone: relationship betweem cone-beam computed tomography and multislice helical computed tomography, Clinical Oral Implants Research, 20: 503-509, 2009.

25. Silva, I. M. C. C., Freitas, D. Q., Ambrosano, G. M. B., et al. Bone density: comparative evaluation of hounsfield units in multislice and cone-beam computed tomography, Brazilian Oral Research, 6: 550-556, 2012.

26. Arisan, V., Karabuda, Z. C., Avsever, H., et al. Conventional multi-slice computed tomography (CT) and cone-beam CT (CBCT) for computer-assisted implant placement. Part I: relationship of radiographic gray density and implant stability. Clinical Implant Dentistry and Related Research, 15: 893-906, 2013.

27. Emadi, N., Safi, Y., Bagheban, A. A., et al. Comparison of CT-number and gray scale value of different dental materials and hard tissues in CT and CBCT. Iranian Endodontic Journal, 9: 283-286, 2014.